REACTIVE CONTROL OF SPATIALLY DEVELOPING TURBULENT BOUNDARY LAYER

Alexander Stroh[1], Yosuke Hasegawa[2] & Bettina Frohnapfel[1]
[1]*Institute for Fluid Mechanics, Karlsruhe Institute of Technology, Germany*
[2]*Institute of Industrial Science, University of Tokyo, Japan*

INTRODUCTION & MOTIVATION

Reduction of losses caused by turbulent skin friction drag is of great economical and ecological interest. One of the promising turbulence control strategies is a reactive control, where instantaneous flow field information captured by sensors is used in order to determine actuator operation. Such control schemes exhibit high energy gain due to low power consumption. Although most previous control schemes have been assessed in fully developed turbulent channel flows, their applicability in spatially developing turbulent flows are not fully investigated. Moreover, previous investigations in boundary layers have so far not considered the control efficiency which can be estimated through evaluation of the power required to run the control. In the present work the control performance of reactive turbulence control is investigated in a turbulent boundary layer and a thorough analysis of the flow state is performed using the FIK-Identity [3] to clarify the drag reduction mechanism.

PROCEDURE

The investigation is performed using direct numerical simulations of a turbulent boundary layer with zero pressure gradient in a Reynolds number range of $\mathrm{Re}_\Theta = 400-750$. In the present investigation opposition control proposed by [2] is considered as a representative of reactive control schemes. The control is applied partially on the wall of the simulation domain by imposing wall-normal velocity opposite to the wall-normal velocity captured at the sensing plane y_s. Correspondingly, the control input at the wall is given by

$$v(x,0,z,t) = -v(x,y_s,z,t). \tag{1}$$

The optimal position is found to be located at y_s = 12, which corresponds to the wall-normal coordinate decaying from y_s^+ = 13 to 11 in viscous units.

Opposition control is applied partially in the streamwise direction, while the spanwise extension of the control area covers the total domain width (Fig. 1). In order to better investigate the control effect downstream of the control section, three control areas with streamwise extension of $\Delta x_c = 100, 150$ and 200 are introduced.

The control performance is estimated through the reduction of skin friction drag with respect to the uncontrolled value [4]. Based on the local driving power

$$P(x) = \bar{\tau}_w(x) U_0, \tag{2}$$

the local drag reduction rate can be defined as

$$R(x) = 1 - P(x)/P_0(x), \tag{3}$$

where $P(x)$ denotes the local pumping power per unit length, τ_w represents the local wall shear stress and the subscript 0 indicates the uncontrolled values. We evaluate the local control input power as the energy flux through the walls caused by the imposed velocity v:

$$P_{in}(x) = \left(\left| \overline{p(x)v(x)} \right| + 0.5 \left| \overline{\rho v(x)^3} \right| \right). \tag{4}$$

The local energy gain is defined as:

$$G(x) = \left(P_0(x) - P(x) \right) / P_{in}(x). \tag{5}$$

The decomposition of skin friction coefficient into contributing parts, also known as FIK-identity [3] is applied. Following this decomposition, the skin friction coefficient for a boundary layer flow is estimated as follows:

$$c_f\,(x) = c_f^\delta + c_f^T + c_f^B. \tag{6}$$

where c_f^δ represents the boundary layer thickness contribution, c_f^T the Reynolds shear stress contribution and c_f^B the boundary layer specific contribution, which consists of a mean convection and a spatial development contribution.

CONTROL PERFORMANCE

The control performance in terms of drag reduction rate shows good agreement with the results of [5]. Figure 2 (left) demonstrates the distribution of $R(x)$ for three control area lengths along the streamwise coordinate within the turbulent region of the flow. The control efficiency gradually increases in the first part of the control area and reaches a saturated state after $120 - 140$ units yielding $R \approx 22 - 23\%$. These local values are comparable with the results known from previous investigations carried out in a channel flow [1].

The local energy gain exhibits a gradual increase up to $G \approx 10$ with following slight decrease down to $G \approx 8$ (Figure 2, right). The energy gain is significantly reduced in comparison to the gain estimated as $G = 35$ in channel flow simulations [6]. This difference arises from the fact that periodic boundary conditions are applied in channel flow simulations while in a boundary layer domain the inflow properties remain unaffected by the outflow.

It is found that the control activation changes the flow properties downstream of the control section, causing a permanent thinning of the boundary layer (Figure 3). Thinner boundary layers possess a higher skin friction coefficient which leads to a skin friction drag increase after the control section (Figure 2, left). It is obvious that the overall control efficiency is therefore dependent on the definition of the integration area.

COMPONENTAL CONTRIBUTION TO C_F

It is found that the reduction of skin friction is mainly caused by the reduction of the turbulent term, c_f^T, and the boundary layer specific term, c_f^B, appearing in the FIK-Identity (Figure 4). The boundary layer contribution, c_f^δ, remains unaffected in the control region. The decrease of the turbulent contribution has the most significant influence on the overall drag reduction rate and is linked to the supression of the turbulent intensity represented by the Reynolds shear stress. The control effect on the boundary layer specific term is quantitatively less pronounced, but still shows a distinct decrease in the control region. The relaxation of this term occurs very rapidly after $\Delta x = 8-10$ with a following overshoot in comparison to the uncontrolled values. In contrary, the turbulent contribution gradient in the section after the control is very moderate, demonstrating a relaxation section of $\Delta x = 70 - 100$.

OUTLOOK

In future, we plan to extend the simulation domain in streamwise direction in order to investigate the influence of control position and Reynolds number on the overall control performance and to derive an analytical relationship between achieved control effects and specified control properties. It is also planned to investigate the mentioned turbulence control scheme in a turbulent boundary layer further with respect to its sensitivity and control performance when factors like the temporal resolution of sensor and actuators, their finite size or noisy sensor signals are considered.

AKNOWLEDGEMENT

The authors greatly acknowledge the support of Dr.-Ing. G. Khujadze and Prof. Dr.-Ing.habil. M. Oberlack at the Chair of Fluid Dynamics and the Cluster of Excellence "Center of Smart Interfaces", TU Darmstadt, Germany.

References

[1] Y. Chang, S. Collis, and S. Ramakrishnan. Viscous effects in control of near-wall turbulence. *Physics of Fluids*, **14**:4069–4080, 2002.

[2] H. Choi, P. Moin, and J. Kim. Active turbulence control for drag reduction in wall-bounded flows. *J. Fluid Mech.*, **262**:75–110, 1994.

[3] K. Fukagata, K. Iwamoto, and N. Kasagi. Contribution of reynolds stress distribution to the skin friction in wall-bounded flows. *Phys. Fluids*, **14**:L73–L76, 2002.

[4] N. Kasagi, Y. Hasegawa, and K. Fukagata. Toward cost-effective control of wall turbulence for skin friction drag reduction. In *ETC 12*, 2009.

[5] M. Pamiès, E. Garnier, A. Merlen, and P. Sagaut. Response of a spatially developing turbulent boundary layer to active control strategies in the framework of opposition control. *Physics of Fluids*, **19**(10):108102–108102–4, 2007.

[6] A. Stroh, B. Frohnapfel, Y. Hasegawa, N. Kasagi, and C. Tropea. The influence of frequency-limited and noise-contaminated sensing on reactive turbulence control schemes. *Journal of Turbulence*, **13**(16), 2012.

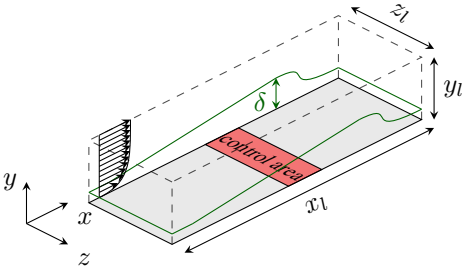

Figure 1. Schematic of the setup

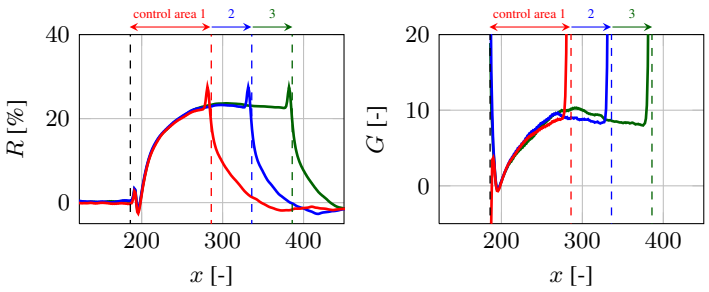

Figure 2. Control performance

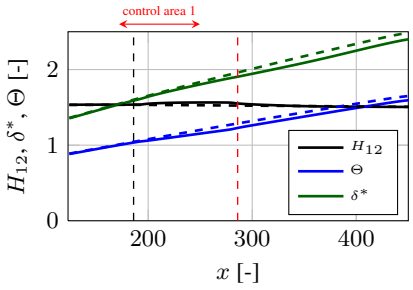

Figure 3. Boundary layer development

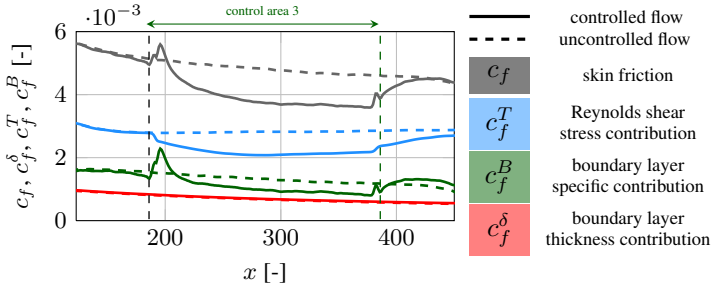

Figure 4. Contribution of FIK-identity components to the skin friction drag